SMOKE VISUALIZATION AND DATA ANALYSIS OF HOT WIRE MEASUREMENTS IN SEPARATED VORTICES OVER AN AXISYMMETRIC PARABOLOID AT HIGH ANGLES OF ATTACK

Tadateru ISHIDE* , Nobuhide NISHIKAWA **
*** Kisarazu National College of Technology, ** Chiba University**

Keywords: *Three Dimensional Separated Flow , Velocity Fluctuation , Hot Wire Anemometer*

Abstract

Various studies of high incidence axisymmetric body have been reported for wide range of Reynolds number, apex angle of a body and so on. Furthermore, the flow patterns of separated region and wake over a body at high angles of attack are relatively complicated. In recent years, for an axisymmetric paraboloid, the extent of longitudinal vortices, such as main-, primary- and secondary vortices, and the change of r.m.s. value in various cross-sections are presented. Additionally, it was shown that the lift-off and mergence of vortices can be explained by r.m.s. distribution of velocity fluctuations. In this study, the flow in the cross-flow separation region of an axisymmetric paraboloid in the angle of attack range from 40 deg to 70 deg was investigated experimentally by smoke visualization technique and hot wire anemometer.

Reynolds numbers range was chosen from 9.0×10^3 to 7.5×10^4 referred to the base diameter. The processes of the change from symmetric to asymmetric vortices and the vortex breakdown were identified on the basis of the visualization results. The relations between a separated vortex and the other flow regions, such as primary separated flow region, reattachment flow region and external flow region, were characterized by calculating two points velocity cross- correlation in various cross-sections. Furthermore, the behavior of each vortex was estimated by calculating the skewness distribution of the velocity fluctuation.

1 Introduction

The flow around a slender body at high angle of attack has been often seen in the field of aerospace, and has been studied from both experiment and numerical analysis [1]. In particular, the data not only in high free stream velocity but also in low free stream velocity have been required in withdrawing and landing of space vehicle. The properties in low free stream velocity are nearly complicated as those in high free stream velocity, and are varied in terms of many parameters, such as angle of attack, Reynolds number, apex angle of axisymmetric body and so on. Furthermore, the flow patterns of separated region and wake over a body at high angles of attack became extremely complicated [2], so those flow patterns cause nonlinearity and singularity of aerodynamic force acting on a body. Therefore, it is of considerable practical significance to understand the properties of the flow qualitatively and quantitatively. From such point of view, the effect of a boundary layer flow for the separated region [3], a geometric definition of the three dimensional separation points , a quantitative definitions of those by measurement of Reynolds stress and wall shear stress have been proposed by several researchers in an axisymmetric body[4][5]. Various studies have been carried out at high angles of attack because separated vortices become asymmetric, and these asymmetric vortices cause significant side forces and yawing moments[6][7]. Additionally, the recent development of visualization technique enabled

the investigation of cross sectional structure of separated vortices in detail [8]. In recent years, for an axisymmetric paraboloid, the authors have reported the measurement of the boundary layer thickness, and assessing the power spectrum of velocity data using a hot wire anemometer which has I-type probe [9]. In the authors' study [10], the three dimensional velocity distribution in the separated vortices over axisymmetric paroboloid was measured in detail using hot wire anemometer having a X-type probe, as a result of this, it was demonstrated that the r.m.s. value of velocity fluctuation has a maximum in the region of secondary vortex near the body surface in the angle of attack range from 30 deg to 50 deg. In the current study [11], the velocity distribution in the separated flow region over an axisymmetric paraboloid was measured in detail using a hot wire so that the distribution of both r.m.s. value of velocity fluctuation and Reynolds stress have been calculated. As a result, the phenomena of the lift-off of longitudinal vortices and the vortex mergence were demonstrated quantitatively. In addition, it was found that the Reynolds stress value fluctuated in the cross section where the vortex core lines became kinky.

2 Experimental setup

The wind tunnel used in this study is the Eiffel type. The test section has a square cross section as 600×600 mm, and length of the section is 650mm. The model was made of stainless steel. This model is an axisymmetric paraboloid, whose radius r is represented by $r=\sqrt{x}$ with x which is the axial distance from the vertex of the model. The nose length L of the model is 140mm, and at the position of x=L diameter D is 75mm. The model is coaxially connected to a 300mm length cylinder as shown in Fig.1.

3 Experimental approach

In this study, two kinds of tracer methods were used as visualization technique. One is injection streak line method for observing the cross section structure of the separated vortices over the model in detail. Another one is smoke wire method for observing the growth of the vortices throughout the model. Argon-ion laser, of which the maximum power is 6w, was used as light source. The beam diameter of laser light is 1.5 mm, and the light sheet whose thickness is 3 mm has been obtained by connecting fiber-link and hemi-cylindrical lens. This light sheet is normal to the body axis.

The hot wire anemometer in this experiment is the type of constant temperature. The average and the fluctuation of the velocity fields around the body have been measured by this apparatus. This measurement system consists of two constant temperature anemometer units and a unit measuring temperature for temperature compensation. A number of division of measuring points in the circumferential direction are nine with equal spacing 11.25° at $90^\circ < \theta < 180^\circ$. In z-direction 20 divisions are selected between the external flow region and the nearest location to the wall which is 0.5mm above the body surface. The procedure for measuring is shown Ref. [11]. In this experiment sampling frequency is 4k Hz, and number of data is 16,384.

4 Results and Discussion

In this experiment, angles of incidence was set in the range from 40 deg to 70 deg. Reynolds numbers are in the range from 9.0×10^3 to 7.5×10^4 referring to 75mm base-diameter at x=L=140mm. The quantitative properties of the

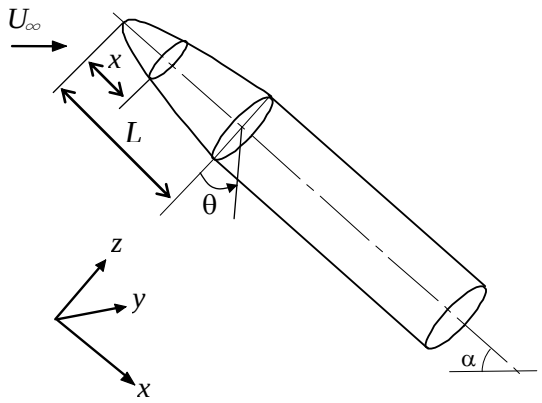

Fig.1 Model and Coordinate system

longitudinal vortices have been investigated. Fig.2 shows visualization picture at 30° of incidence angle, Re=9.0 × 10^3, x/L=1.0. This picture is obtained by the authors' visualization experiments [10]. Main, primary, secondary and tertiary vortices are formed in the region from symmetry line of leeward side to circumferential windward side. The direction of rotation of the adjacent vortices is reversal each other. The longitudinal vortices are generated interactively after main vortex has formed by the separated flow originated with the primary separation line and the reattachment flow from the symmetric line of leeward side.

4.1 Visualization experiments

Fig.3 shows the visualization pictures of the flow around the model using smoke wire method. Fig.3(a) shows the visualization picture at α=40°, Re=1.8×10^4. From this picture, it is confirmed that the boundary line between the separated vortex region and the external flow gradually lifts off the body surface with going downstream side. The location of the boundary line at x/L=1.0 is denoted as P_A, here Z_A/D is 0.208. The mark of P_B shows that tracer indicates meandering near body surface. This phenomenon corresponds to the fluctuating of the secondary vortex core [10]. Fig.3(b) shows the visualization picture at α =50°, Re=1.8 × 10^4. The location of the boundary line at x/L=1.0 is denoted as P_C, here Z_C/D is 0.361 which is 1.73 times Z_A/D. Fig.3(c) shows the visualization picture at α =60°, Re=9.0 × 10^3. It is observed that the boundary line between the separated vortex region and the external flow have extended sharply at location P_D. It is considered that this behavior of tracer corresponds to main vortex breakdown. Fig.3(d) shows the

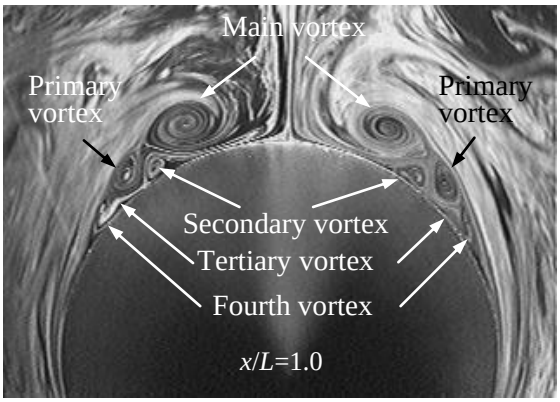

Fig.2 Visualization picture using fog machine (α=30°, Re=9.0×10^3)

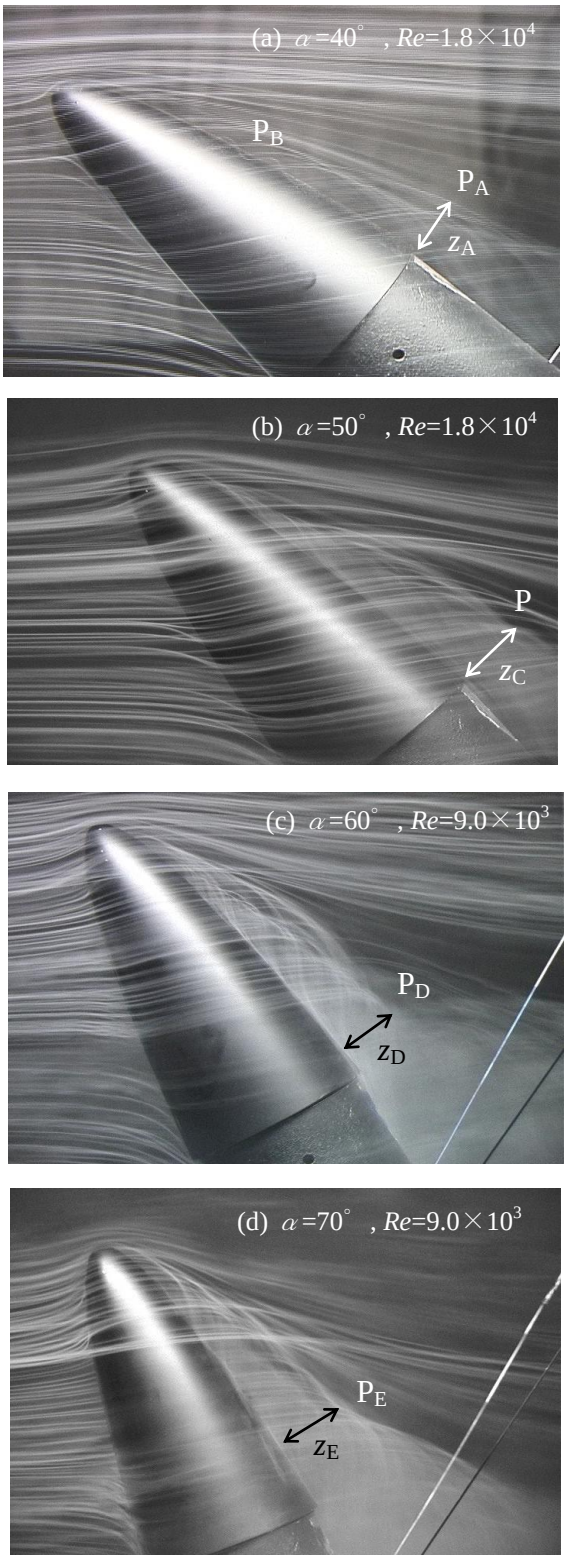

Fig.3 Visualization pictures by smoke wire method

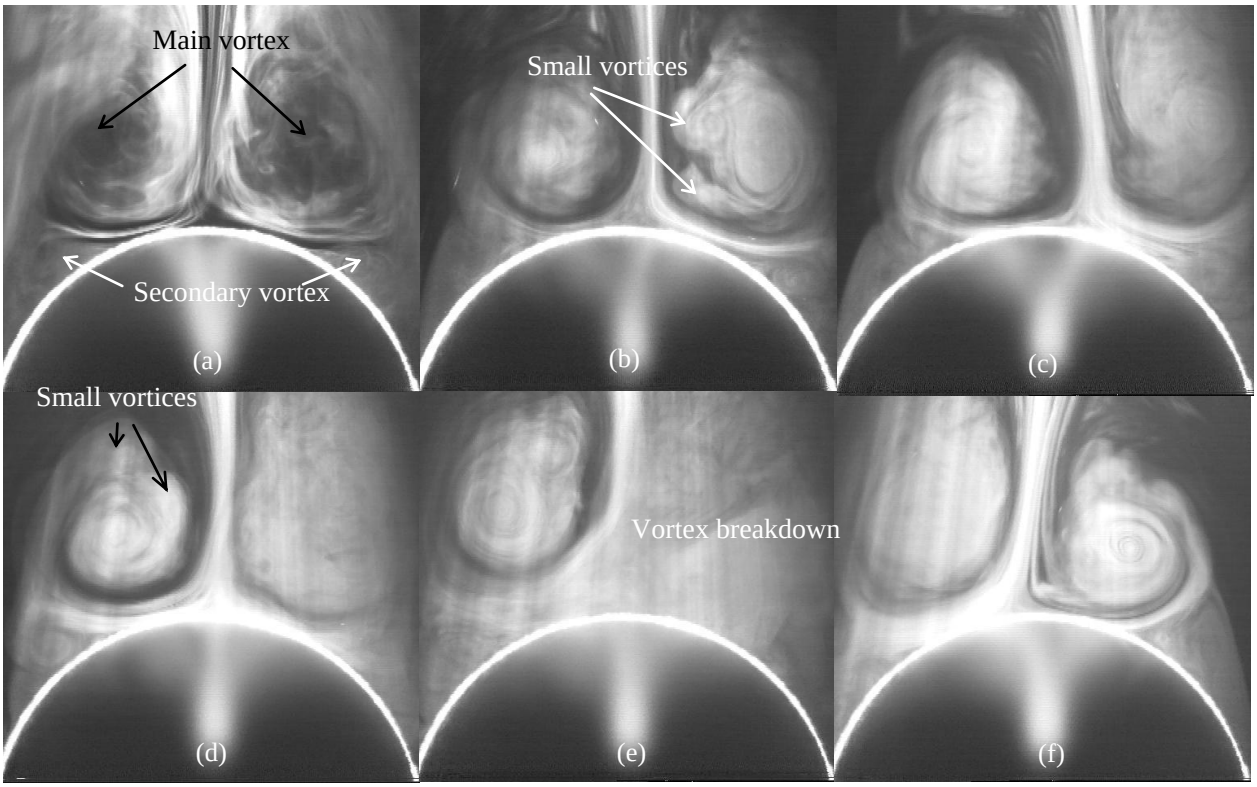

Fig.4 Temporal variation of separated vortex pattern(α=70° ,*Re*=9.0×10^3 , *x*/*L*=1.0)

visualization picture at α=70° , *Re*=9.0×10^3. The abrupt expansion of the separated vortex region can be confirmed at location P_E as same as P_D. Comparing location between P_E and P_D, it is found that the separated vortex at α=70° lifts farther off body surface than α =60° , furthermore the starting point of vortex breakdown moves upstream with respect to the body axis.

Fig.4 shows the temporal variation of separated vortex pattern at α=70° , *Re*=9.0× 10^3. The nearly symmetrical main and secondary vortices can be observed in Fig.4(a). It is confirmed that the small vortices generate in the main vortex after primary vortex merged with secondary vortex, as a consequence of this, the merged vortex was incorporated into the main vortex in Fig.4(b). The most of reattachment flow from the external flow region runs into the separated vortex region at the right area of body symmetry line so that the separated vortices become asymmetric in Fig.4(c). This inclined reattachment flow was caused because the main vortex merged with primary and secondary vortices, as a consequent of this, the circulation at the right area of body symmetry line became stronger than the left area. The mergence of the vortices at the left area of body symmetry line can be validated in Fig.4(d), so the most of reattachment flow from the external flow region runs into the separated region at the left area of body symmetry line. As a result, the main vortex breakdown at the right area of body symmetry line occurs because the vorticity of the separated vortex was weakened in Fig.4(e). It is identified that the separated vortex region at the left area of body symmetry line grows largely in Fig.4(f).

4.2 Hot wire measurements

4.2.1 Two-points velocity cross- correlation

In this study, the two points velocity cross correlation in various cross-sections was calculated to clarify the relations between the separated vortices and the other flow regions, such as the region near primary separation line, the reattachment flow region and the external

flow region. The two points velocity cross correlation was evaluated as follows.

$$R_{AB}(\tau) = C_{AB}(\tau) / \left(\sqrt{\overline{A^2}} \sqrt{\overline{B^2}} \right) \quad (1)$$

$$C_{AB}(\tau) = \overline{A(t)B(t+\tau)} = \lim_{T\to\infty} \frac{1}{T} \int_{-T/2}^{T/2} A(t)B(t+\tau)dt \quad (2)$$

Here, we denote A as the reference point in main, primary and secondary vortices, which is obtained by velocity vectors in each cross section. Fig.5 shows the synthesized image of visualization picture and velocity vectors at α =40° , Re=1.8 × 10^4, x/L=0.86. From this figure, we can recognize V_1 as measured velocity in the primary vortex, V_2 as in the secondary vortex. The measuring time interval τ is 0.00025 sec, and the sampling time T is 2.048 sec in Eq. (1) and (2).

Fig.6 shows the contour of two points velocity correlation R_{AB} at α=40° , Re=1.8× 10^4 in case that a measured velocity in the main vortex region at x/L=0.43 is set as reference point A. The R_{AB} values near reference point A are relatively high at x/L=0.43. The high R_{AB} values appear also at the point B_{61} of which coordinate is θ=157.5° , z/R_1=1.14 (R_1: radius of cross section at x/L=0.43) in the main vortex region. At x/L=0.79, B_{62} in the external flow region and B_{63} in the main vortex region have high R_{AB} values respectively. In addition, B_{64} near body surface at 135° <θ<157.5° shows low R_{AB} values. The region B_{65} containing low R_{AB} values become extended into the range of 112.5° <θ<163° . This result was caused by the large temporal variation of velocity because the turbulence in the secondary vortex region generates with propagating to the main vortex region in the downstream side of the body. Moreover, the reattachment region B_{66} has high R_{AB} values which is closer to body surface than B_{62} at x/L=0.79. At x/L=1.0, the low R_{AB} region enlarges in the range from body surface to z/R_4=0.77 (R_4: radius of cross section at x/L=1.0). Especially, the region B_{67} occupying between the primary vortex and the main vortex at 112.5 ° <θ<146.3 ° , and the secondary vortex region B_{68} show low R_{AB} values. These results are expected to be related to the phenomenon that the primary and the secondary vortices were incorporated into the main vortex. Furthermore, the R_{AB} values are high in the region near the primary separation line in all cross sections at θ=90° .

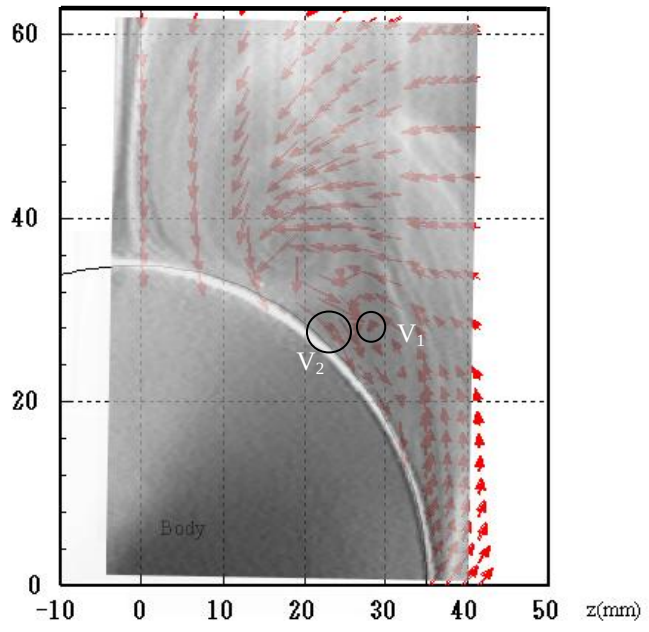

Fig.5 Synthesized image of visualization picture and velocity vectors(α=40° , Re=1.8×10^4, x/L=0.86)

Fig.7 shows the contour of two points velocity correlation R_{AB} at α=50° , Re=1.8× 10^4 in case that a measured velocity in the main vortex region at x/L=0.32 is set as reference point A. The high R_{AB} value regions are dotted in the cross section at x/L=0.32, therefore the reattachment region B_{71} and the outer edge of the main vortex region B_{72}, B_{73} show high R_{AB} values. The reattachment region B_{74} and the region B_{75} near the primary separation line at x/L=0.43 also show high R_{AB} values as nearly same as those at x/L=0.32 so that the behaviors of the separated vortices agree with α=40° . In addition, the low R_{AB} value region starts to extend in the main vortex region. At x/L=0.71, the low value region further enlarges, as a consequence this, it can be stated that this region occupies with most of the main vortex region. It is confirmed that the relatively high R_{AB} values appear in the reattachment region. The location B_{76} which has maximum R_{AB} value 0.34, appears at θ=168° ,

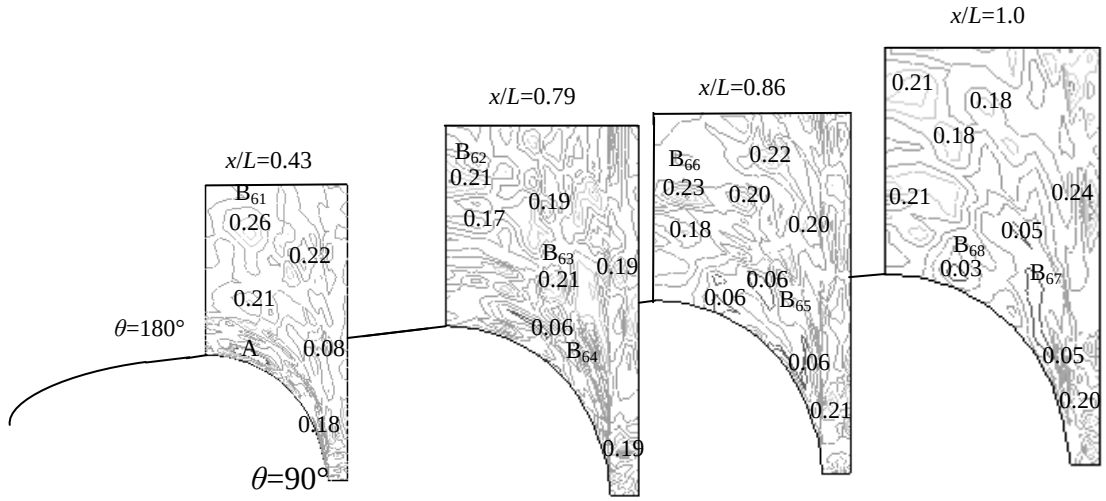

Fig.6 Two points velocity correlation contour (α=40° , Re=1.8×10^4)

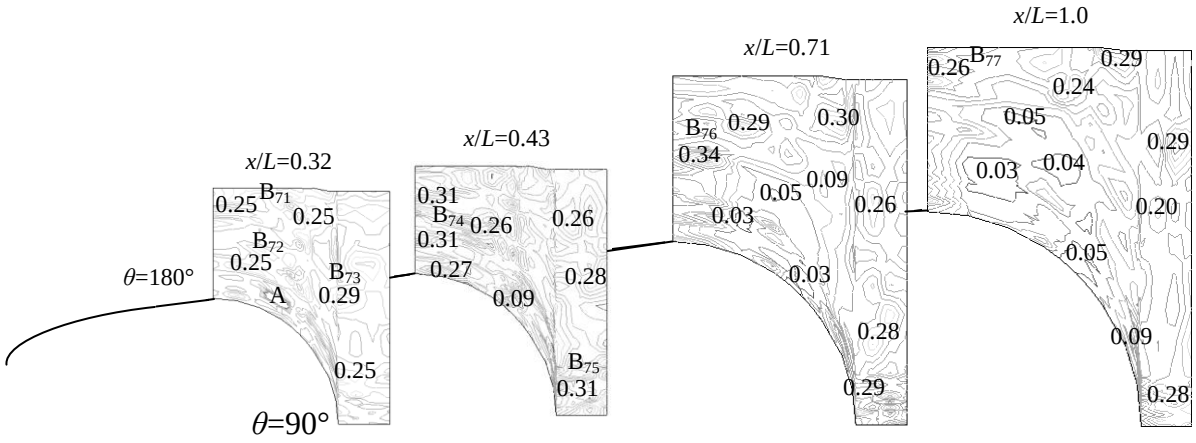

Fig.7 Two points velocity correlation contour (α=50° , Re=1.8×10^4)

z/R_6=0.49 (R_6: radius of cross section at x/L=0.71), so it is conjectured that the part of fluid particles in the main vortex lifted off in the result of incorporating the primary vortex. This tendency is notable at x/L=1.0, that is, the main vortex lifted off the body surface with intensity of the turbulence, as a consequence of this, the part of the main vortex moves to the external flow region acting a free vortex.

4.2.2 Skewness distribution

In this study, we noted a skewness value which is one of turbulence statistic representing a distribution condition for measured velocity to track the behavior of separated vortices in detail. Skewness is a measure of the asymmetry of the probability distribution in time-series measuring velocity data.

Fig.8 shows the contour of skewness distribution in each cross section at α=40° , Re=1.8 × 10^4. From this figure, the primary vortex P and the secondary vortex S can be recognized in the range from x/L=0.43 to 0.86. It was confirmed that both the primary vortex and secondary vortex are incorporated into the main vortex at x/L=1.0. Fig.9 shows the contour of skewness distribution in each cross section at α =50° , Re=1.8 × 10^4. The primary vortex P and main vortex M can be identified at x/L=0.32, 0.43, 0.71, 1.0. On the other hand, the primary vortex can not be recognized at x/L=0.57 because the sweep flow appeared which is blowing to the body surface from the external flow region [10]. The mergence between the primary P vortex and the main vortex M can be confirmed on the leeward of the cross section at x/L=0.71.

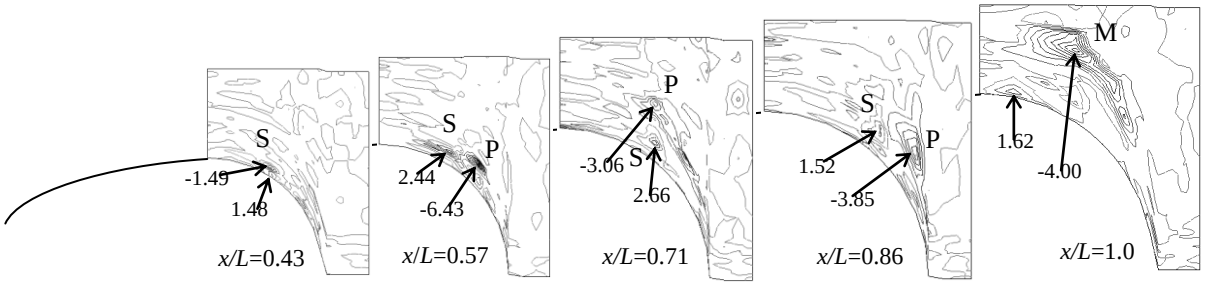

Fig.8 Contour of skewness distribution in each cross section (α=40°, Re=1.8×10^4)

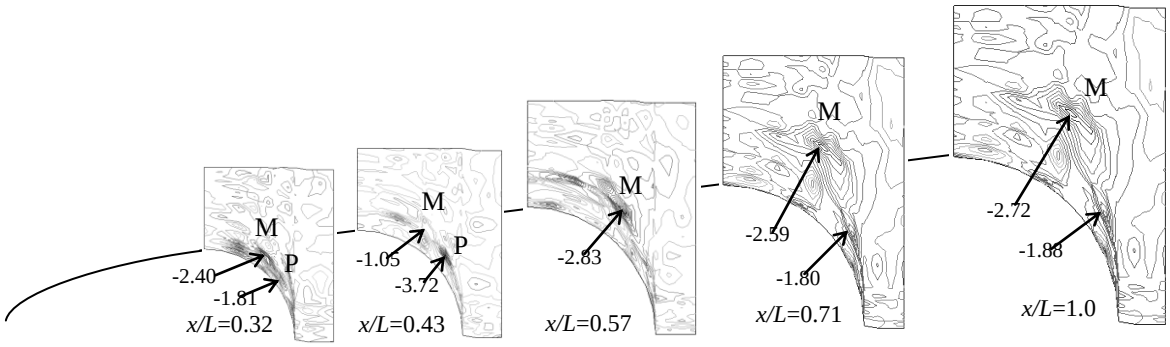

Fig.9 Contour of skewness distribution in each cross section (α=50°, Re=1.8×10^4)

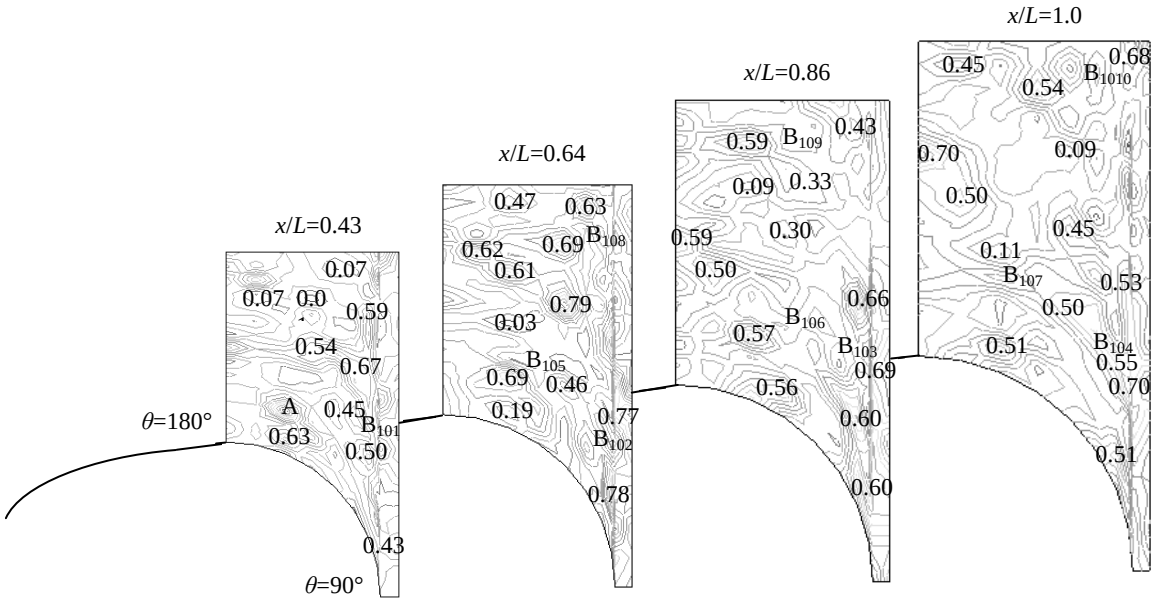

Fig.10 Two points velocity correlation contour (α=60° , Re=9.0×10^3)

4.2.3 Effect of angle of attack and Reynolds number

Fig.10 shows the contour of two points velocity correlation R_{AB} at α=60° , Re=9.0×10^3 in case that a measured velocity in the main vortex region at x/L=0.43 is set as reference point A. From this figure, it may be stated that the regions B_{101}~B_{104} which is occupying the region from the primary separation line to the outer edge of the main vortex have high R_{AB} values in all cross sections. The maximum R_{AB}

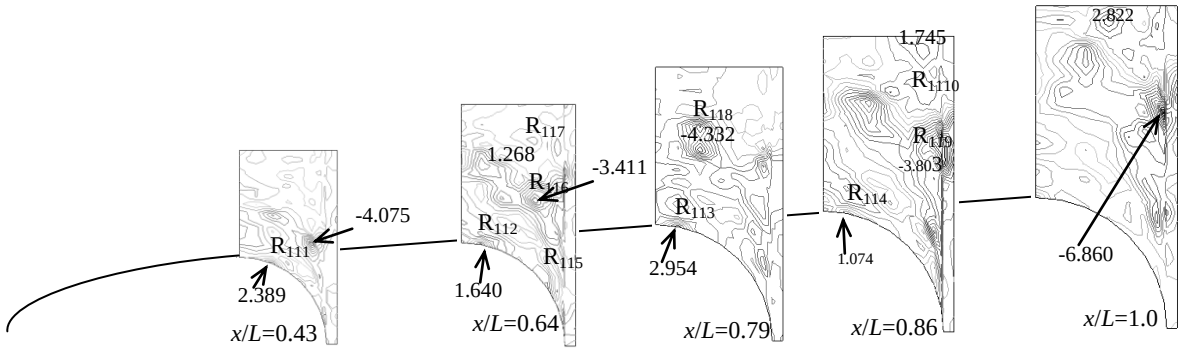

Fig.11 Contour of skewness distribution in each cross section (α=60°, Re=9.0×10^3)

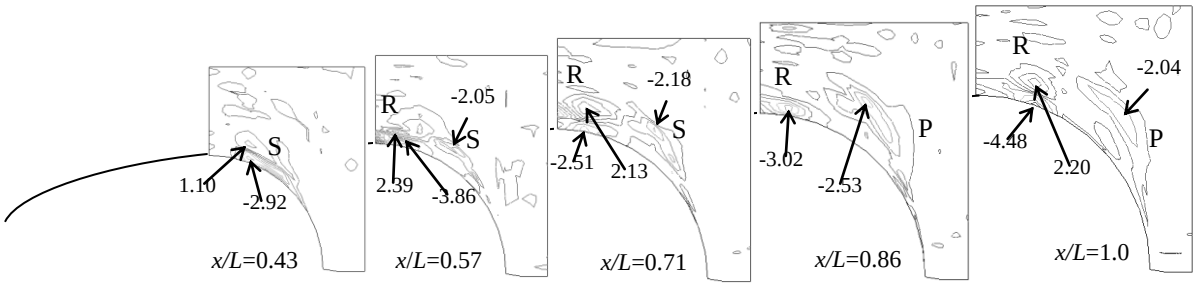

Fig.12 Contour of skewness distribution in each cross section (α=40° , Re=7.5×10^4)

value is about two times that of α=40° , it would appear that a two dimensional flow separating from the primary separation line is mainly appearing. Although the R_{AB} values near the main vortex core B_{105}, B_{106} at x/L=0.64 and 0.86 show high R_{AB} values, this value decreases one-fifth at B_{107} at x/L=1.0. It is attributed to the main vortex breakdown between x/L=0.86 and 1.0. In addition, the locations of large R_{AB} values move above shown in B_{108}~B_{1010} with the extending of the separated vortex region. It is considered that these locations show the boundary between the separated vortex and the external flow region.

Fig.11 shows the contour of skewness distribution in each cross section at α=60° , Re=9.0 × 10^3. From this figure, the high values in the reattachment regions R_{111}~R_{114} in the range from x/L=0.43 to 0.86 can be confirmed. The primary vortex has been incorporated into the main vortex at the region R_{115} at x/L=0.64. The region R_{116} near the outer edge of the main vortex and R_{117} in the external flow region also have high absolute values. These values are related to the generation of small vortices at x/L=0.79 as the same what we observed in the visualization experiments as above mentioned. The high absolute values show in the outer edge of the main vortex R_{118} at x/L=0.79 with the generation of the small vortices. At x/L=0.86, the region R_{119} adjacent to the high (rms×dfn) region [11] and R_{1110} in the external flow region show the high absolute skewness values also. These values are explained by the main vortex breakdown at x/L=1.0.

Fig.12 shows the contour of skewness distribution in each cross section at α=40° , Re=7.5 × 10^4. The absolute skewness values are high in the reattachment regions R near the body surface in all cross sections. This is attributable to the intermittent secondary separation. From this figure, it can be found that the secondary vortex moves to the main vortex in the cross section range from x/L=0.43 to 0.71, while the primary vortex moves to the main vortex behind x/L=0.86.

5 Conclusions

In this study, we have investigated the separated vortices over axisymmetric paraboloid at high angles of attack. The following conclusions were derived from the results and discussion.

(1)The development of flow pattern from symmetric separated vortices to asymmetric those has been clarified by the visualization technique using fog generator and laser light sheet.

(2)The main vortex breakdown is much affected by the reattachment flow, that is, this phenomenon has generated after the direction of the reattachment flow had changed.

(3)It can be concluded that the two points velocity correlation values between each separated vortex and the region near primary separation line or the reattachment flow region are relatively high, on the contrary, those values are low in the region where the mergence of separated vortices occurred.

(4)The locations of each separated vortex were specified by calculating the skewness of time-series of acquired velocity data at α=40, 50 deg. As a result, the differences of the enlarging process with respect to the angles of attack are found.

References

[1] Erickson G.E. High Angle-of-Attack Aerodynamics. *Annu. Rev. Fluid Mech.*, Vol.**27**, pp 45-88, 1995.

[2] Jia M, Watanuki T and Kubota H. The Visualization of Separated Flow over Slender Bodies at High Angles of Attack. *J.Visualization Soc. Jpn.*, Vol.14, No.55, pp 243-252, 1994.

[3] Barberis D and Molton P. Experimental Study of Three-Dimensional Separation on a Large-Scale Model. *AIAA J.*, Vol.33, No.11, pp 2107-2113, 1995.

[4] Kreplin H.P and Stager R. Measurements of the Reynolds-Stress Tensor in the Three-Dimensional Boundary Layer of an Inclined Body of Revolution. *Proc. 9th Symp. "TURBULENT SHEAR FLOWS"*, Kyoto, pp 2.4.1-2.4.6, 1993.

[5] Chesnakas C.J and Simpson R.L. Measurements of the Turbulence Structure in the Vicinity of a 3-D Separation. *Trans. ASME*, Vol.118, pp 268-275,1996.

[6] Ericsson L.E and Reding J.P. Vortex-Induced Asymmetric Loads in 2-D and 3-D Flows. *AIAA Paper*, 80-0181, 1980.

[7] Champigny P G. Stability of Side Forces on Bodies at High Angles of Attack. *AIAA Paper*, 86-1776, 1986.

[8] Degani D and Zilliac G.G. Experimental Study of Nonsteady Asymmetric Flow around an Ogive Cylinder at Incidence. *AIAA J.*, Vol.28, No.4, pp 642-649, 1990.

[9] Ishide T and Nishikawa N. Experimental Study of Unsteady Flow behavior in Separated Flow along Blunt Body. *Proc. 31st Aircraft Symp.*, Tokyo, pp 140-143, 1993.

[10] Ishide T, Nishikawa N and Mikami F. Experimental Investigation of Three Dimensional Separated Flow over a Body of Revolution at High Angles of Attack, *CD-ROM Proc. 22nd Int. Congress Aeronaut. Sci.*, Harrogate, pp 293.1-293.9, 2000.

[11] Ishide T, Nishikawa N and Mikami F. Clarification of Unsteady Characteristics in Separated Flow over an Axisymmetric Paraboloid at High Angles of Attack, *CD-ROM proc. of 23rd International Congress of Aeronautical Sciences*, Toronto, pp 3113.1-3113.12, 2002.

Copyright Statement